Hydrol. Earth Syst. Sci. Discuss., doi:10.5194/hess-2016-290, 2016
Manuscript under review for journal Hydrol. Earth Syst. Sci.
Published: 20 June 2016

Hydrology and Earth System Sciences
Discussions

Water budget modelling of the Upper Blue Nile basin using the JGrass-NewAge model system and satellite data

Wuletawu Abera[1], Giuseppe Formetta[2], Luca Brocca[3], and Riccardo Rigon[1]

[1]Department of Civil, Environmental and Mechanical Engineering, University of Trento, Italy
[2]Centre for Ecology & Hydrology, Crowmarsh Gifford, Wallingford, UK
[3]Research Institute for Geo-Hydrological Protection, National Research Council, Perugia, Italy

Correspondence to: Wuletawu Abera (wuletawu979@gmail.com); Riccardo Rigon(riccardo.rigon@ing.unitn.it)

Abstract. The Upper Blue Nile basin is one of the most data-scarce regions in the world, hence, the hydrological information required for informed decision making in water resources management is limited. The hydrological complexity of the basin, tied with the lack of hydrometerological data, means that most hydrological studies in the region are either restricted to small subbasins where there are relatively better hydrometeorological data available, or at the whole basin scale but at very coarse time scales and spatial resolutions. In this study we develop a methodology that can improve the state-of-art by using the available, but sparse, hydrometerological data and satellite products. To this scope, we use the JGrass-NewAGE system to estimates the water budget components (Precipitation J, Evapotranspiration ET, discharge Q, and storage ds/dt). The satellite products SM2R-CCI is used for obtaining the rainfall inputs; SAF EUMETSAT for cloud cover fraction for proper net radiation estimation; GLEAM for comparison with estimated ET; and GRACE gravimetry data also for comparison of the total water storage amounts available. Results are obtained at daily time-steps for the period 1994-2009 (16 years), and they can be used as a reference for any water resource development activities in the region. The overall long term mean budget analysis shows that precipitation of the basin is 1360 $\pm$230 mm per year. Evaporation covers 56% of the yearly budget, runoff is 33%. Storage varies from minus 9.7% to plus 6.9% of the budget.

Key Words: Water budget, Upper Blue Nile, JGrass-NewAGE system, Satellite data, evapotranspiration

1 Introduction

Freshwater is a scarce resource in many regions of the world: the problem continues to be aggravated by growing populations and significant increases in demand for agricultural and industrial purposes. The Nile River basin is one such region, with relatively arid climate because of high temperatures and solar radiation, which foster rapid evapotranspiration. Most of the countries within the basin, such as Egypt, Sudan, Kenya, and Tanzania, receive insufficient fresh water (Pimentel et al., 2004). Exceptions to this are the small areas at the equators and the Upper Blue Nile basin in the Ethiopian highlands, which receives up to 2000 mm per year (Johnston and McCartney, 2010). Particularly, the Upper Blue Nile (hereafter UBN) basin is the main sources of water in the region. Also, it is probably one of the most hydro-climatologically and socio-politically complex basins in the world. The water resources in the basin faces many pressures and challenges: (1) as the principal contributor (i.e 85%) to the main Nile basin, it supports the lives of hundreds of millions of people living downstream, and it is referred to as the "Water Tower" of northeast Africa; (2) locally, the basin is inhabited by 20 million people whose main livelihood is subsistence agriculture (Population Census Commission 2008); (3) topographically, the basin is very complex: it starts from mountains as high as 4,300 m asl and drains to lowlands of about 450 m asl; (4) the UBN is a part of trans-boundary river, hence its development and management require diplomatic discussions with many national governments; (5) many international and non-governmental organizations, each with different policies, legal regimes, and contrasting interests, are involved in the freshwater governance of the basin; (6) the Ethiopian government has started many water resource development projects, such as irrigation schemes and dams, among which the Grand Ethiopia Renaissance Dam (GERD), which, upon completion, will be one of the largest in Africa.

Tackling all these complexities and challenges and developing better water development strategies is only possible with quantitative information (Hall et al., 2014) of the hydrological system. Understanding the hydrological processes of the basin, therefore, is the basis for both the transboundary negotiations about sharing the water resources of the basin (FAO 2000) and for assessing the sustainability of subsistence farming systems in the region. Because of the lack of hydrometeorological data and a proper modelling framework, however, the recent modelling efforts conducted within the basin have their limitations in addressing these problems. As a consequence, spatio-temporal hydrological information in the basin is very scarce. Studies in the region are limited to small basins, particularly within the Lake Tana basin where there are relatively better hydrometeorological data (Rientjes et al., 2011; Uhlenbrook et al., 2010; Tekleab et al., 2011; Wale et al., 2009; Kebede et al., 2006; Bewket and Sterk, 2005; Steenhuis et al., 2009; Conway, 1997; Mishra et al., 2004; Mishra and Hata, 2006; Teferi et al., 2010), or at the whole basin scale, but in which case information on spatial variability is usually ignored (Kim et al., 2008; Kim and Kaluarachchi, 2009; Gebremicael et al., 2013; Tekleab et al., 2011). Other studies are limited to a specific hydrological process e.g. rainfall variability (Block and Rajagopalan, 2007; Abtew et al., 2009), time series and statistical analysis of in situ discharge/rainfall data (Teferi et al., 2010; Taye and Willems, 2011) or modelling at very low temporal resolutions (e.g. monthly) (Kim and Kaluarachchi, 2008; Tekleab et al., 2011). Consequently, spatially distributed information on all the components of the water budget does not exist. In a region where all the hydrological fluxes (precipitation, evapotranspiration and discharge) are important elements of the water budget, "traditional" basin modelling approaches that are tailored to a single component do not provide a complete picture of the dynamics of the water resources within the basin.

Large scale, data-sparse, hydrological modelling can be supported by remote sensing (RS) products, which fill the data gaps in water balance dynamics estimation (Sheffield et al., 2012). The use of RS precipitation products in hydrological applications can be found elsewhere in literature (Hong et al., 2006; Bellerby, 2007; Huffman et al., 2007; Kummerow et al., 1998; Joyce et al., 2004; Sorooshian et al., 2000; Brocca et al., 2014). Effective utilization of different RS products is clearly a new paradigm in water budget closure estimations (Sheffield et al., 2009; Andrew et al., 2014; Sahoo et al., 2011; Gao et al., 2010; Wang et al., 2014).

This study is an effort to contribute to the aforementioned problems and aims to resolve the water budget of the UBN basin using a hydrological modelling framework and remote sensing data. It is also a methodological paper, in that it delineate various methodologies to overcome the data scarcity, and inherits from Abera et al. 2016.

The paper is organized as follows: firstly, descriptions of the study area and model setup are given(section 2), then the methodologies for each water budget component and the model set-up are detailed in section 3. The results and discussions of each component and the water budget are presented in section 5. Finally, the conclusions of the study are given (section 6).

2 The Study Basin

The Upper Blue Nile (UBN) river originates at Lake Tana at Bahir Dar, flowing southeast through a series of cataracts. After about 150 km, the river enters a deep a canyon, and at the same slowly change direction south. After flowing for another 120 km flow, the river again changes its direction to the west and northwest, towards the El Diem (Ethiopia-Sudan border). Many tributaries draining from many parts of the Ethiopian highlands join the main river along its course. The total distance of the river within Ethiopia is about 1000 km.

The UBN basin represents up to 60% of the Ethiopian highlands contribution to the Nile river flows, which is itself 85% of the total (Abu-Zeid and Biswas, 1996; Conway, 2000). The area of the river basin enclosed by a section at the Ethiopia-Sudan border is about 175,315 km^2 (figure 1), covering about 17% of the total area of the country. The large scale hydrological behaviour of the basin is described in a series of studies (Conway, 1997, 2000, 2005; Conway and Hulme, 1993). Specifically, its hydrological behaviour is characterized by high spatio-temporal variability. Since the UBN basin has the lion's share of the total Nile flow, it is the economic mainstay of downstream countries (i.e. Sudan and Egypt). Moreover, the Ethiopian highlands are highly populated and have high water demands of their own for irrigation and domestic uses.

The topographic distribution of the basin is shown in figure 1. The topography of UBN is very complex, with elevation ranging from 500 m in the lowlands at the Sudan border to 4160 m in the upper parts of the basin. Due to the topographic variations, the climate of the basin varies from cool (in the highlands) to hot (in the lowlands), with large variations in a limited elevation range. The hot season is from March to May, the wet season, with lower temperatures, is from June to September, while the dry season runs from October to February. There are three controlling mechanisms of rainfall in the UBN basin and in Ethiopia as whole (Seleshi and Zanke, 2004): the Intertropical Convergence Zone (ITCZ) that drives the monsoon rainfall during the wet season (Jun.-Sept.); the Saharan anticyclone that generates the dry and cool northeasterly winds in the dry season (Oct.-Feb.); and the Arabian highlands that produce thermal lows in the hot season (Mar.-May). Specifically studies have found that the interannual and seasonal variability of precipitation in the UBN basin is governed by the Southern Oscillation Index (SOI), the equatorial eastern Pacific sea level pressure, and the sea-surface temperature (SST) over the tropical eastern Pacific Ocean (Camberlin, 1997; Seleshi and Zanke, 2004). The mean annual rainfall and potential evapotranspiration of the UBN basin are estimated to be in the ranges of 1,200-1,600 mm and 1,000-1,800 mm, respectively (Conway, 1997, 2000), with high spatio-temporal variability. The annual temperature mean is 18.5^o, with small seasonal variability. Generally, the seasonal variability of the basin is very high.

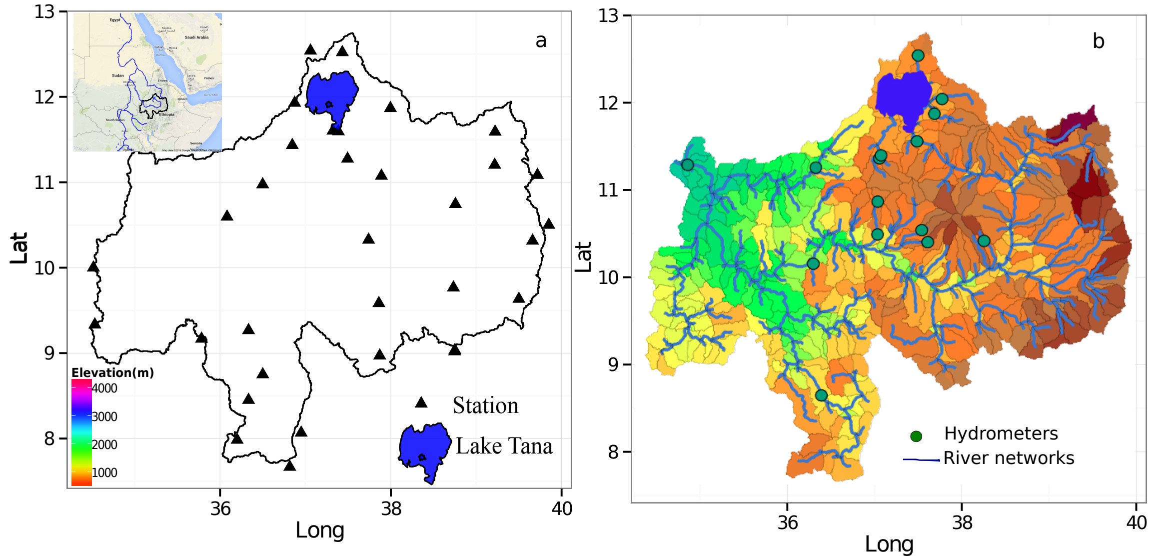

Figure 1. The Upper Blue Nile basin digital elevation map, along with the meteorological stations (a); and subbasin partitions and hydrometers used for simulation (b).

3 Methodology

3.1 Water Budget modelling

Water budget simulation is essential to the estimation of both water storage and water fluxes (rate of flow) for given, appropriate, control volumes and time periods. It is given by:

$$\frac{\partial S_k(t)}{\partial t} = J_k(t) + \sum_{i}^{m(k)} Q_{ki}(t) - ET_k(t) - Q_k(t) \tag{1}$$

where $J(t)$ is rainfall, and $ET(t)$ is actual evapotranspiration, $Q(t)$ is discharge, $Q_{ki}(t)$ is the discharge from the contributing streams. The index $k = 1,2,3...$ is the control volume where the water budget is solved. In our case, the control volume is a portion of the basin (a subbasin) derived from topographic partitioning as described in section 3.2. Different RS and in situ data are used to enforce or validate the modelling solutions implemented and to close the water budgets. The datasets used for the water budget are described in their respective sections.

3.2 JGrass-NewAGE system set-up

The JGrass-NewAGE hydrological model system is used to resolve the water budget of the UBN basin. JGrass-NewAGE is a set of modelling components that can be connected at runtime (Formetta et al., 2014b) to create various modelling solutions. The JGrass-NewAGE system (Formetta et al., 2011) and the various individual components are described in a series of papers (Formetta, 2013; Formetta et al., 2014c, 2013, 2011, 2014b, a; Abera et al., 2014), and are not re-discussed here. In this study, the solar radiation budget (SWRB), the evapotranspiration component (Priestley and Taylor), the Adige rainfall-runoff model, and all the components illustrated in figure 2 are used to estimate the various hydrological flows .

A necessary step for spatial hydrological modelling is the partitioning of the topographic information into an appropriate spatial scale. The GIS representation of the basin topography, as detailed in (Formetta et al., 2014a; Abera et al., 2014; Formetta et al., 2011), is based on the Pfafstetter enumeration (Formetta et al., 2014a; Abera et al., 2014). The basin is subdivided in Hydrologic Response Units (HRUs), where the model inputs (i.e. meteorological forcing data), and hydrological processes and outputs (i.e. evapotranspiration, discharge, net radiation) are averaged. The water budget components are estimated for each HRU and, subsequently, a routing scheme is applied to move the discharges to the basin outlet through the channel network.

In this study, the UBN basin is divided into 402 subbasins and channel links, as shown in figure 1b. This spatial partitioning may not be the finest scale possible, however, considering the size of the basin, it can be considered an acceptable scale to capture spatial variability of the water budget.

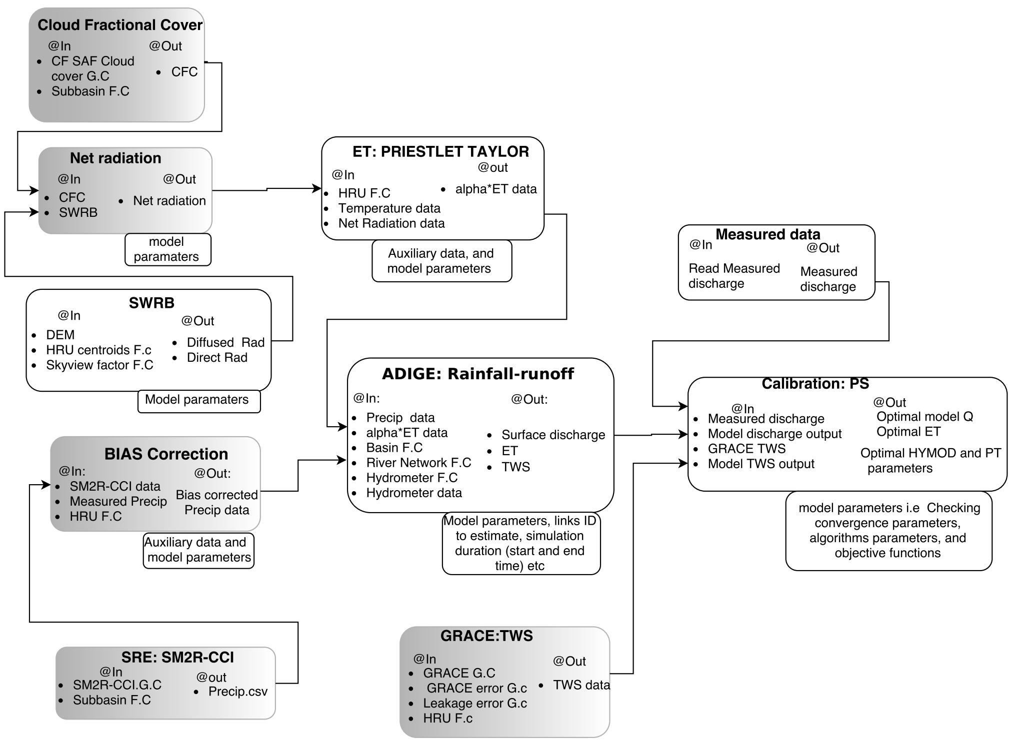

Figure 2. Workflow with a list of NewAge components (in white), and remote sensing data processing parts (shaded in grey, not yet included in JGrass-NewAGE and currently performed with R tools) used to derive the water budget of the UBN. It does not include the components used for the validation and verification processes.

Hydrol. Earth Syst. Sci. Discuss., doi:10.5194/hess-2016-290, 2016
Manuscript under review for journal Hydrol. Earth Syst. Sci.
Published: 20 June 2016

3.2.1 Precipitation $J(t)$

The spatio-temporal precipitation input term of Eq. 1 (J(t)), is quantified with RS-based approaches. Currently, there are several satellite rainfall estimates (SREs) available for free that are characterized by varying degrees of accuracy and reliability. Recently Abera et al. (2016) compared five potentially good SREs with high spatial and temporal resolutions in a series of hydrological applications for the same basin. It was shown that SM2R-CCI (Brocca et al., 2013, 2014) is one of the best products, particularly in capturing the total rainfall volume. A comparative analysis of the effects of different SREs on basin water budget is an interesting area of research that can be extended from this study, however, here only SM2R-CCI is used as water budget modelling input. The systematic error (bias) of SM2R-CCI is removed according to the ecdf matching techniques Michelangeli et al. (2009); Abera et al. (2016).

Once SM2R-CCI is corrected for bias errors, it is used to examine the spatio-temporal precipitation variability of the basin and drive the JGrass-NewAGE modelling system to solve the discharge. The subbasin mean precipitation is estimated by averaging all the pixels within each subbasin. In accordance with the basin partition described in section 3.2, the 1994-2009 daily precipitation set is generated for 402 subbasins.

3.2.2 Evapotranspiration ET

The evapotranspiration component, is crucial for agricultural and water resources management as it is an important flux within a basin. The lack of in-situ data relating to ET impedes modelling efforts and makes it probably the most difficult task in water budget estimation. Here, ET is formulated according to the NewAge evapotranspiration component using the radiation budget as input, as it is the main radiant energy available at the surface to drive the surface biophysical processes and evapotranspiration (Kjaersgaard et al., 2009). This approach provides estimates at any temporal and spatial resolution required. The Priestley and Taylor (PT) Formula (Priestley and Taylor, 1972) is one of the simplified models used to estimate ET. It is mainly based on net radiation, Rn, simplifying all the unknowns into the α coefficient, as shown in Eq. 2.

$$ET = \alpha \frac{\Delta}{\Delta + \gamma}(Rn) \tag{2}$$

Where Δ is the slope of the Clausius-Clapeyron relations and γ is the psychometric constant (Abera et al., submitted). In this study, however, the actual evapotranspiration, ET is constrained not only by the atmospheric demands estimated using PT (Eq. 2), but it uses storage information which can be obtained from the ADIGE rainfall-runoff component of JGrass-NewAGE. Hence, the ET equation is modified as:

$$ET(t) = \alpha \frac{S(t)}{S_{max}} \frac{\Delta}{\Delta + \gamma}(Rn) \tag{3}$$

The important unknown coefficient α (Pejam et al., 2006; Assouline et al., 2016) and the S_{max} (maximum water storage capacity for each HRU) are calibrated within the rainfall-runoff model component, as explained below. In this procedure, given that S(t) is not measures, the assumption that there is null water storage difference after a long time, named Budyko′s time, TB, (Budyko, 1978), is required. Once it is fixed, automatic calibration can be set to produce the set of parameters, including α for which, besides discharge is well reproduced, also $S(t) = 0$ after T_B. In this study, $T_B = 6$ years.

In equation 3, Rn is the main input modulating the atmospheric demand component of ET. The NewAge shortwave radiation budget component, SWRB (Formetta et al., 2013), is used to estimate the shortwave radiation budget for each subbasin in clear sky conditions. Irradiance in clear sky conditions, however, is unsuitable for all sky condition. Surface shortwave radiation is strongly affected by cloud cover and cloud type (Arking, 1991; Kjærsgaard et al., 2009). Therefore, the clear sky SWRB estimated using NewAge-SWRB is cut to Rn in all-sky conditions by using the cloud fractional cover (CFC) satellite data set (Karlsson et al., 2013), processed and provided by EUMETSAT Climate Monitoring Satellite Application Facility (CM SAF) project (Schulz et al., 2009). In this case net radiation is generated only from the shortwave radiation and the cloud cover data, as in the following formulation (Kim and Hogue, 2008):

$$Rn = (1 - CFC)R_S \tag{4}$$

Where R_S is the net shortwave radiation estimated using the NewAge-SWRB component for each subbasin, and Rn is the net radiation. The daily CFC data originates from polar orbiting satellites, version CDRV001, using a daily temporal resolution and a 0.25^o spatial resolution from 1994 to 2009 (16 years). Satellite data are processed (Karlsson et al., 2013) to obtain the mean daily CFC for each subbasin. In comparison to CFC, the effects of surface albedo on Rn is minimal, particularly in highland areas with vegetation cover and no snow cover such as the UBN basin.

Once ET is estimated according to the methods described, it is useful to validate it with independently obtained ET estimates or data. In situ ET observations are not available for this basin, as is the case for most regions. Estimates of ET based on RS have been made by different algorithms (Norman et al., 1995; Mu et al., 2007; Jarmain, 2009; Fisher et al., 2008). In this study, the Global Land Evaporation Amsterdam Methodology (GLEAM) (Miralles et al., 2011a), a global, satellite-based, ET data set is used. The performance of GLEAM is assessed positively in different studies (McCabe et al., 2016; Miralles et al., 2011b). GLEAM is available at 0.25^o spatial resolution and daily temporal resolution. Differently from the NewAge approach, GLEAM also considers dynamic vegetation information to cut PT-based potential ET to actual ET (Miralles et al., 2011a). The aim of the comparison is not for strict validation, but rather to assess the level of consistency between the two independent estimations. More details on GLEAM can be found in Miralles et al. (2011a, b); McCabe et al. (2016). Comparison of the NewAge ET with MODIS standard ET product is also available in the supplementary material of the paper.

3.2.3 Discharge *Q*

For discharge estimation, the ADIGE rainfall-runoff component is used. It is based on the well-known HYMOD model (Moore, 1985). The main inputs for the ADIGE model are $J(t)$ and $ET(t)$, as estimated in the previous sections. Detailed descriptions of HYMOD implementations in the NewAge model system are given at Formetta et al. (2011) and Abera et al. (submitted). The ADIGE rainfall-runoff has five calibration parameters, and the calibration is performed using the particle swarm (PS) optimization. PS is a population-based stochastic optimization technique inspired by the social behaviour of flocking birds or fish schools (Kennedy et al., 1995). It is suited to obtaining a global optimal and less susceptible to getting trapped in local minima (Scheerlinck et al., 2009). The objective function used to estimate the optimal value of the parameter is the Kling-Gupta efficiency (Kling et al., 2012). The KGE is preferred to the commonly-used Nash-Sutcliffe efficiency (NSE, Nash and Sutcliffe (1970)) because the NSE has been criticized for its overestimation of model skill for highly seasonal variables by underestimating flow variability (Schaefli and Gupta, 2007; Gupta et al., 2009). For evaluation of the model performances, in addition to the KGE, two other goodness-of-fit (GOF) methods (percentage bias (PBIAS) and correlation coefficient) used in this study are described in A.

3.2.4 Total water storage change ds/dt

The ds/dt in Eq. 1 is the water contained in the ground, soil, snow and ice, lakes and rivers, and biomass. It is the total water storage (TWS) change, calculated as the residuals of the water budget fluxes for each control volume. In this paper, the ds/dt estimation at daily time steps is based on the interplay of all the other components as presented in Eq. 1. There is no way to estimate areal TWS from in situ observations. The new Gravity Recovery and Climate Experiment (GRACE) data (Landerer and Swenson, 2012) has a potential to estimate this component, but at very low spatial and temporal resolutions. At large scale, however, it can still be used for constraining and validating data to the modelling solutions. Here, the performance of our modelling approach to close the water budget, i.e. estimating storage following the characterization of all the terms, is assessed using the GRACE estimation at the basin scale. Monthly data is obtained from NASA's Jet Propulsion Laboratory (JPL) ftp:// podaac-ftp.jpl.nasa.gov/allData/tellus/L3/land mass/RL05. The leakage errors and scaling factor (Landerer and Swenson, 2012) that are provided with the product are applied to improve the data before the comparison is made. The total error of GRACE estimation is a combination of GRACE measurement and leakage errors (Billah et al., 2015). Based on the data of these two error types, the mean monthly error of GRACE in estimating total water storage change (TWSC) in the basin is about 8.2 mm. Since the other fluxes, for instance Q and ET, are modelled as functions of basin water storage, the good estimation of water storage by a model has inference to its reasonable computation of other fluxes as well (Döll et al., 2014).

4 Calibration and validation approach

The satellite precipitation data set (SM2R-CCI) is error corrected based on in situ observations. The ADIGE rainfall-runoff component (i.e. HYMOD model) is calibrated to fit the observed discharge during the six years of calibration period (1994-1999) at daily time steps. Based on the approach described in the ET estimation section, PT α is calibrated by searching for $S(t)$ to be null after $T_B = 6$ years. The value of six years is arbitrary but it was found to give good agreement with GRACE data (see below), so no other values were used. The simulation for each hydrological component is then verified using available in-situ or remote sensing data as follows:

– Discharge validation: Discharge simulation is validated for separate time-series data at the outlet at Ethiopian-sudan Border, where the model is calibrated. In addition, the simulation of NewAge at the internal links is validated where

Hydrol. Earth Syst. Sci. Discuss., doi:10.5194/hess-2016-290, 2016
Manuscript under review for journal Hydrol. Earth Syst. Sci.
Published: 20 June 2016

in situ data are available. The evaluations at the internal links provide an assessment of model estimation capacity at ungauged locations.

- ET validation: Once ET is estimated according to the procedures described above, GLEAM (Miralles et al., 2011a) is used as an independent data set to assess ET estimation. After GLEAM is aggregated for each subbasin, the GLEAM and the NewAge ET are compared and the goodness-of-fit (GOF) indexes are calculated, based on 16 years of data (1994-2009).

- ds/dt validation: The water storage change, ds/dt, estimated as residual of the water budget is validated against the GRACE based data-set. The GRACE product was used to estimate the total water storage change for the the whole basin, since the error of GRACE increases if used at small scales. To harmonize and enable comparison between the model and the GRACE TWS data, it is necessary to do both time and spatial filtering. Following the GRACE TWSc temporal resolution, the model ds/dt is aggregated at monthly time steps.

5 Results and Discussion

The results of the study are organized as follows: Firstly, we present the results for simulation performance and their comparison with independent data, along with brief spatio-temporal characteristics of the fluxes and storage. The simulated water budget components are described in the following order: 1) precipitation; 2) evapotranspiration; 3) discharge; and 4) total water storage. Secondly, the components are used to resolve the water budget closure at each subbasin, hence, the contribution of each term is analyzed.

5.1 Precipitation J

The spatial distribution of mean, long-term, annual precipitation is presented in figure 3a. SM2R-CCI shows that the south and southwest parts of the basin receives high precipitation while the east and northeast parts of the highlands receive low precipitation. The rainiest subbasins are in the southern part of the basin in the Oromia region. The precepitation data used gives these subbasins a mean annual rainfall of about 1900 mm, while the mean annual precipitation reported for this region by Abtew et al. (2009) is about 2049 mm. The small discrepancy could be that the Abtew et al. (2009) estimation is from point gauge data, while in this study it is based on the areal data from SM2R-CCI, corrected by available ground rain gauges. Generally, precipitation increases from the east (about 1000 mm/year) to the south and southwest (1800 mm/year). This spatial pattern is consistent with the results of Mellander et al. (2013) and Abtew et al. (2009). To understand the spatial distribution of the seasonal cycle, the quarterly percentage of total annual precipitation, calculated from 1994 to 2009 in daily estimations, is presented in figure 3 b. During the summer season (June, July and August), while the subbasins in the north and northeast receive about 65% (figure 3 b), the subbasins in the south receive about 40% of total precipitation.

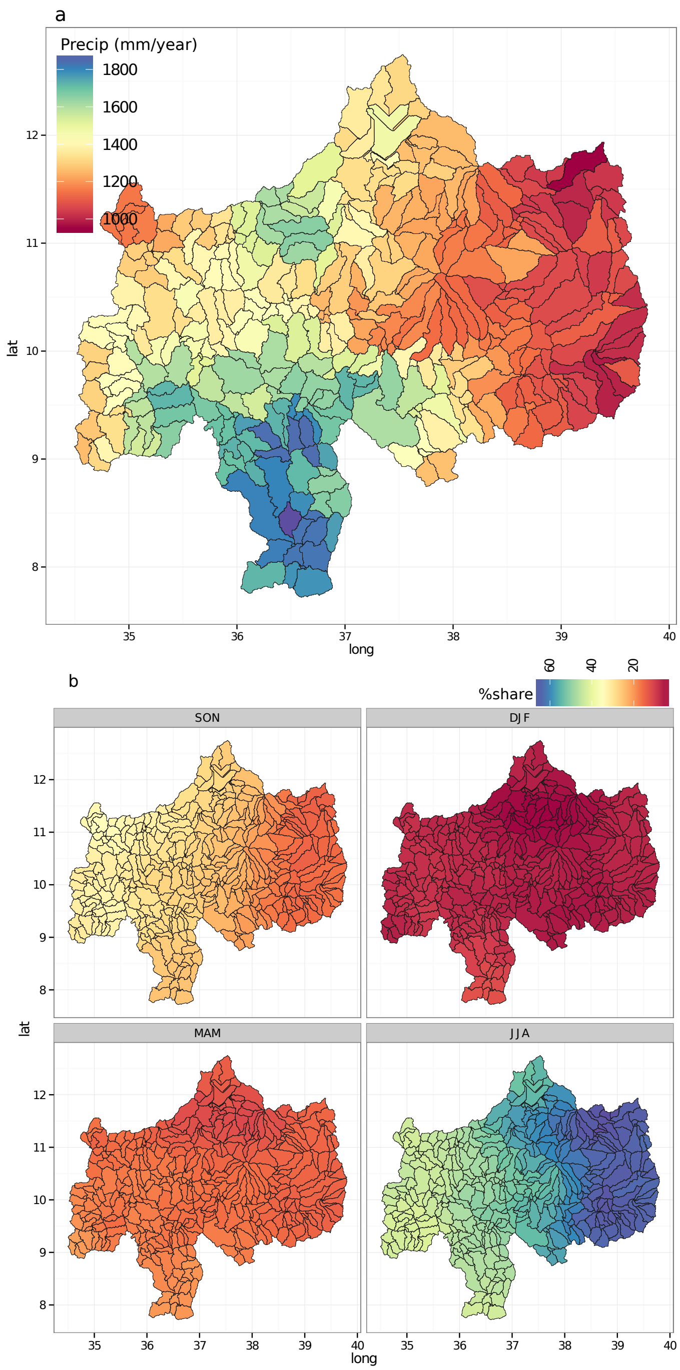

Figure 3. The spatial distribution of mean annual rainfall (a), and quarterly percentages share of the total rainfall (b) estimated from long term data (1994-2009). SON (September, October, and November), DJF(December, January, and February), MAM (March, April, and May), JJA (June, July and August).

Hydrol. Earth Syst. Sci. Discuss., doi:10.5194/hess-2016-290, 2016
Manuscript under review for journal Hydrol. Earth Syst. Sci.
Published: 20 June 2016

5.1.1 Evapotranspiration *ET*

Based on the approach detailed in our methodology, the ET is estimated for each subbasin at daily time steps. A comparison of time series (three time steps i.e. daily, weekly, and monthly) of the two ET estimations (NewAge and GLEAM), from 1994-2002 and for some selected subbasins, is shown in figure 4 a. NewAge revealed high levels of temporal variability in comparison to GLEAM for all three time steps. It clearly shows that GLEAM underestimates ET during the peak periods and overestimates it during low periods.

The agreement between the two estimations varies from subbasin to subbasin (figure 4). The spatial distribution correlation and PBIAS between the NewAge and GLEAM ET is presented in figure 4 b. Generally, the correlation between the two ET estimations increases when passing from daily to monthly time steps. Spatially, the correlation is higher in the eastern and central part of the basin, while the it tends to decrease systematically towards the west (i.e. to the lowlands, see figure 4 b). Regarding the PBIAS maps, there is no significant difference between the three time steps. The PBIAS between the two ranges from -10% to 10%, with large numbers of subbasin being from -3% to 3%. Spatially, the comparison shows that NewAge underestimate ET in the western parts of the basin (border to the Sudan) and overestimates ET in the northern parts of the basin (figure 4b). The overall basin correlation is 0.34 $\pm$ 0.07 (daily time step), 0.51 $\pm$ 0.08 (weekly time step), and 0.57 $\pm$ 0.10 (monthly time steps). The PBIAS does not change over the three time steps (1.5 $\pm$ 9.1%). Generally, except at daily time step, the two estimates have acceptable agreements (very low bias, and acceptable correlation). In comparison to the correlation (0.48 $\pm$ 0.15) and PBIAS (14.5 $\pm$ 18.9%) obtained with the comparison between NewAge ET and MODIS ET Product (MODET16) at 8-days time steps, the correlation and PBIAS between NewAge ET and GLEAM ET is much better (supplementary material).

5.1.2 Discharge *Q*

The automatic calibration of the NewAge components provided very good values of the GOF indices (KGE=0.93, PBIAS = 2.2, r = 0.94). At the same location, model performance is verified during the validation period and it is almost equal to the performance during the calibration period. Model performance is also evaluated within the basin at the internal channels (2). Figure 5 shows simulated hydrographs for some channel links, when available, along with the observed discharge. At the outlet, even during the validation period, the model is able to capture the dynamics of the basin response very well (KGE=0.92, PBIAS = 2.4, r = 0.93). The results show that the performances of the NewAge simulation are similar to the performances reported by Mengistu and Sorteberg (2012), with slightly lower PBIAS value (PB=8.2, r^2=0.92). Generally, the model predicts both the high flows and low flows well, with slight underestimation of peak flows (figure 5 a), which is likely due to the underestimation of SM2R-CCI precipitation data for high rainfall intensities (Abera et al., 2016).

For further analysis and understanding of the NewAge discharge forecasting capacity, model goodness-of-fit for some internal sites are described here. For the Gelgel Beles river, enclosed at the bridge near to Mandura with an area of 675 km^2, the hydrograph comparison between the NewAge simulated discharge and the observed one is shown in figure 5 b. The perfor-

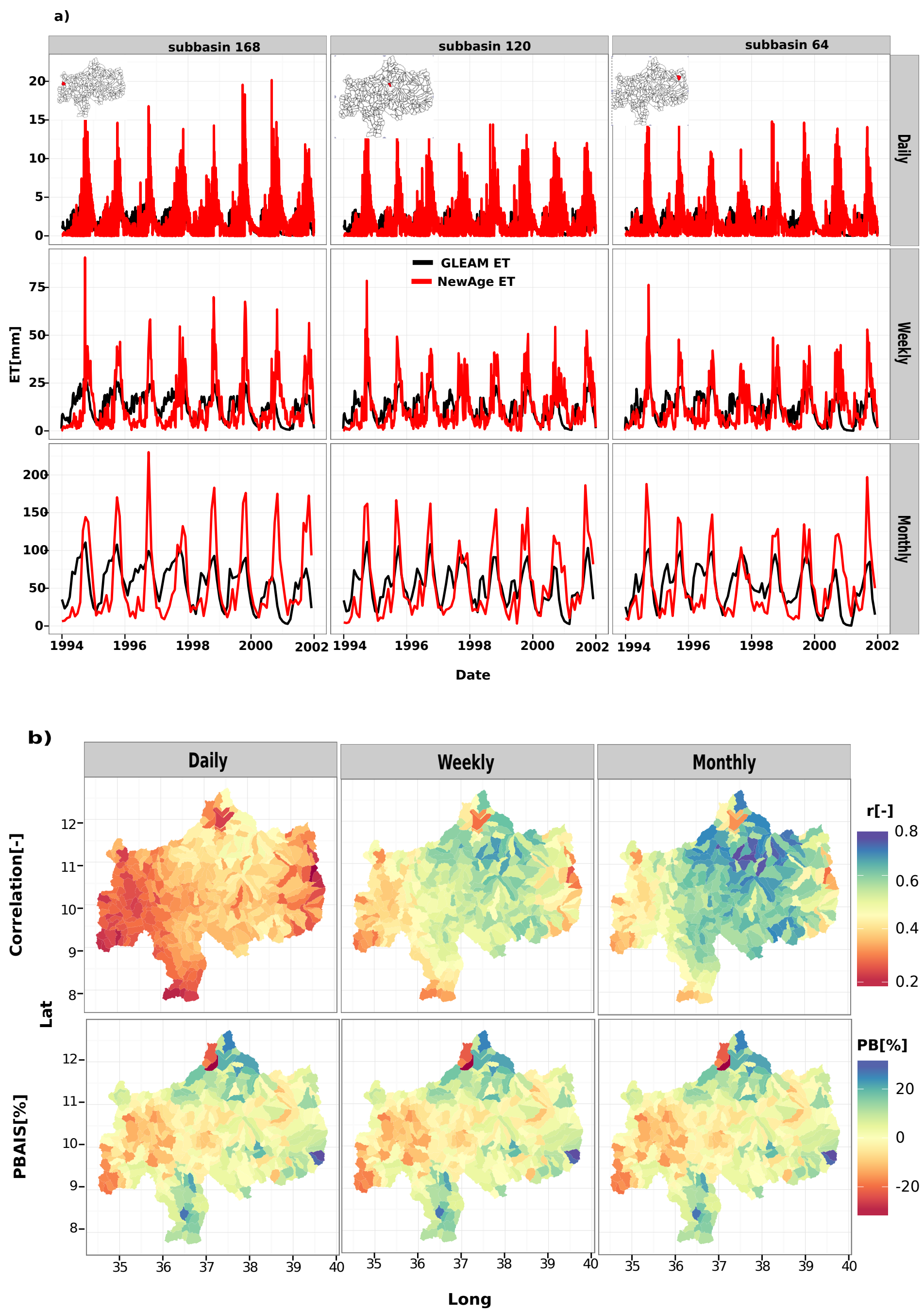

Figure 4. a:Time series ET estimation with NewAge and GLEAM for three subbasins: subbasin ID168 , subbasin ID120, and subbasin ID64 at daily, weekly and monthly time steps. The locations of the subbasins are indicated on the maps at the top of each column of plots. b: spatial distribution of correlation coefficient and PBIAS between NewAge and GLEAM estimations at daily, weekly and monthly time steps.

Hydrol. Earth Syst. Sci. Discuss., doi:10.5194/hess-2016-290, 2016
Manuscript under review for journal Hydrol. Earth Syst. Sci.
Published: 20 June 2016

Hydrology and Earth System Sciences
Open Access
Discussions

Table 1. Optimized parameters obtained from daily ADIGE simulation during the calibration period (1994-1999). The last parameter is for the ET component.

Parameters	value
$C_{max}[L]$	694.18
$B_{exp}[-]$	0.64
$\alpha[-]$	0.61
$Rs[T]$	0.086
$Rq[T]$	0.394
$\alpha[-]$	2.9

Table 2. The forecasting capacity of the NewAge Adige rainfall-runoff component at the internal sites, based on the optimized parameters calibrated at the outlet. The performance at the outlet (El Diem) is the model performance during validation period.

River Name (Hydrometer stations)	Area (km^2)	KGE	PBIAS	r
Koga @ Merawi	244.00	0.67	-8.70	0.73
Jedeb @ Amanuel	305.00	0.38	40.80	0.53
Suha @ Bichena	359.00	0.54	39.20	0.82
Temcha @ Dembecha	406.00	0.70	3.30	0.71
Gilgel Beles @ Mandura	675.00	0.68	11.40	0.70
Lower Fettam @ Galibed	757.00	0.67	-7.7	0.78
Gummera @ Bahir Dar	1394.00	0.19	-53.20	0.88
Ribb @ Addis Zemen	1592.00	0.81	12.00	0.86
Gelgel Abay @ Merawi	1664.00	0.81	12.00	0.93
Main Beles @ Bridge	3431.00	0.68	-1.70	0.74
Little Anger @ Gutin	3742.00	0.65	24.30	0.81
Great Anger @ Nekemt	4674.00	0.72	-14.10	0.82
Didessa @ Arjo	9981.00	0.55	19.60	0.81
Upper Blue Nile @ Bahir Dar	15321.00	0.26	5.10	0.60
Upper Blue Nile @ El Diem	174000.00	0.92	2.40	0.93

Hydrol. Earth Syst. Sci. Discuss., doi:10.5194/hess-2016-290, 2016
Manuscript under review for journal Hydrol. Earth Syst. Sci.
Published: 20 June 2016

mance of the uncalibrated NewAge at Gelegel Beles has a correlation coefficient of 0.70, PBIAS is 11.40% and the KGE value is 0.68 (Table 2).

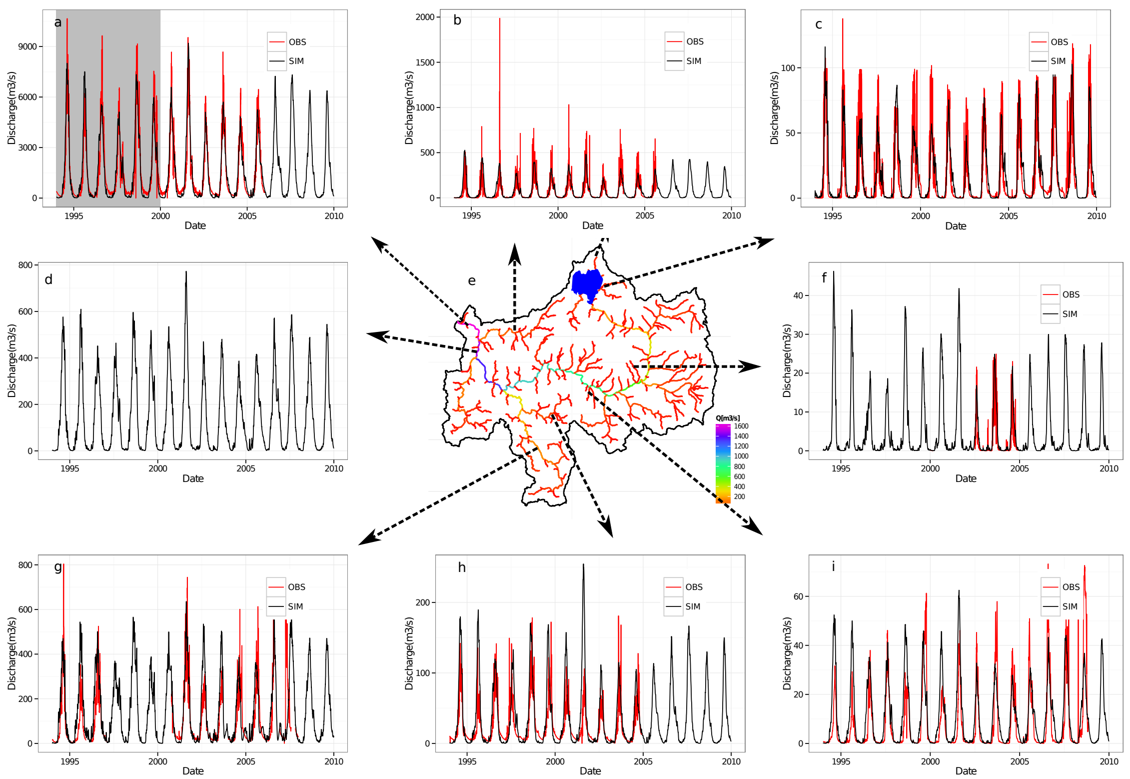

Figure 5. NewAge model forecasting validation at internal subbasins. The model calibrated and validated at El Diem (a) is used to estimate at each channel link and, where discharge measurements are available, they are verified: main Beles bridge (b), Ribb river enclosed at Addis Zemen (c), just simulation of the main Blue Nile before joining Beles river (d), Jedeb near Amanuel (f), Dedisa river basin enclosed near Arjo (g), Angar river basin enclosed near Nekemt (h), and Nesh near Shambu (i). Figure (e) shows the long term estimated daily discharge for all river links of the basin.

Simulation performances for the medium size basins, based on model parameters calibrated at basin outlet, such as the Ribb river, enclosed at Addis Zemen (area=1592 km^2, KGE = 0.81, PBIAS = 12% and r = 0.82, figure 5 c), and Gilgel Abay river, enclosed at Merawi (area = 1664 km^2, KGE=0.81, PBIAS=12%, r=0.93), are very good. For the Ribb river, the NewAge simulation performance can be compared with SWAT Model performances by (Setegn et al., 2008) (R^2=0.55-0.57). Even though SWAT was calibrated for this specific subbasin, the results of our study are much better. Similarly, without calibration for the Gilgel Abay river, the NewAge simulation performance is comparable with the results of Wase-Tana (PBIAS=34), SWAT (PBIAS=5) and Flex$_B$ (PBIAS=77.6), sometimes even better (Wosenie et al., 2014).

To analyze the forecasting capacity of NewAge for the larger size basins, the performances at Angar river (area 4674 km^2), Lake Tana (area 15321 km^2), and Dedisa river basin (9981 km^2) are reported. The simulation analysis at the Angar river

Hydrol. Earth Syst. Sci. Discuss., doi:10.5194/hess-2016-290, 2016
Manuscript under review for journal Hydrol. Earth Syst. Sci.
Published: 20 June 2016

enclosed near Nekemt (KGE = 0.72, PBIAS = -14.10%, and r = 0.82), Lake Tana (KGE = 0.26, PBIAS = 5.10, and r = 0.60), and Dedisa (KGE=0.55, PBIAS = 19.60, and r = 0.81) indicate that the performances are acceptable. The comparison of simulated and observed discharges, as well as the locations of the Angar (basin brief description (Easton et al., 2010)) and Dedisa rivers are shown in figure 5, in plots h and g respectively.

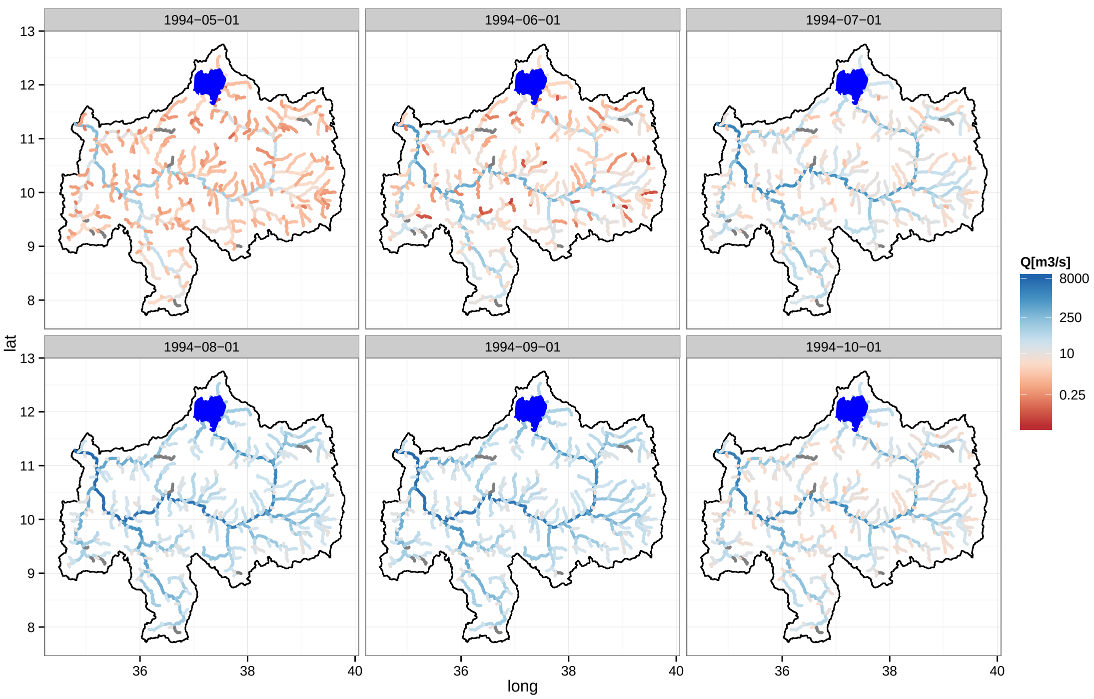

Figure 6. The spatial distribution of simulated discharge for each link of the basin at daily time steps. Here, the spatial distribution of discharge is shown for the first day of May, June, July, August, September, and October of 1994.

For most subbasins, because of the good model performances (i.e. KGE is higher than 0.5 and PBIAS is within 20%), the estimated discharges are deemed adequate for forecasting and estimating water resource at locations where gauges are unavailable. The model is also able to reproduce discharge across the range of scales. For instance, the model performances at the Ethiopia-Sudan border (175 315 km^2), Dedisa near Arjo (9981 km^2), main Beles (3431 km^2), and Temcha near Dembecha (406 km^2) are also acceptable (figure 5 and table 2).

A sample of spatially distributed daily discharge at all the channel links is shown in figure 6. Here, the daily discharge for the first day of May, June, July, August, September and October are presented to show the spatio-temporal dynamics of discharge.

Hydrol. Earth Syst. Sci. Discuss., doi:10.5194/hess-2016-290, 2016
Manuscript under review for journal Hydrol. Earth Syst. Sci.
Published: 20 June 2016

5.1.3 Total water storage change

The NewAge simulated ds/dt for 16 years for each subbasin, calculating it as a residual of the flux terms. We first compared the simulated ds/dt with GRACE-based TWSC. Figure 7 shows ds/dt time series for the whole basin, estimated by using NewAge and GRACE. The storage change shows high seasonality over the basin, with positive change in summer and negative change in winter. The change varies from -100 to +120 mm/month. The model ds/dt, aggregated at monthly time scale, is in accordance with the GRACE TWSC both in temporal pattern and amplitude. Over the whole basin a correlation coefficient of 0.84 is obtained. The good performances of the ds/dt component also has an inference on the model capability to reproduce other components well, as it is the residual terms that balance the flux dynamics.

Due to the possible high leakage error introduced at high spatial resolutions (Swenson and Wahr, 2006), statistical comparison at subbasin level is not performed.

The spatial distribution of NewAge and GRACE ds/dt can be found in the complimentary material.

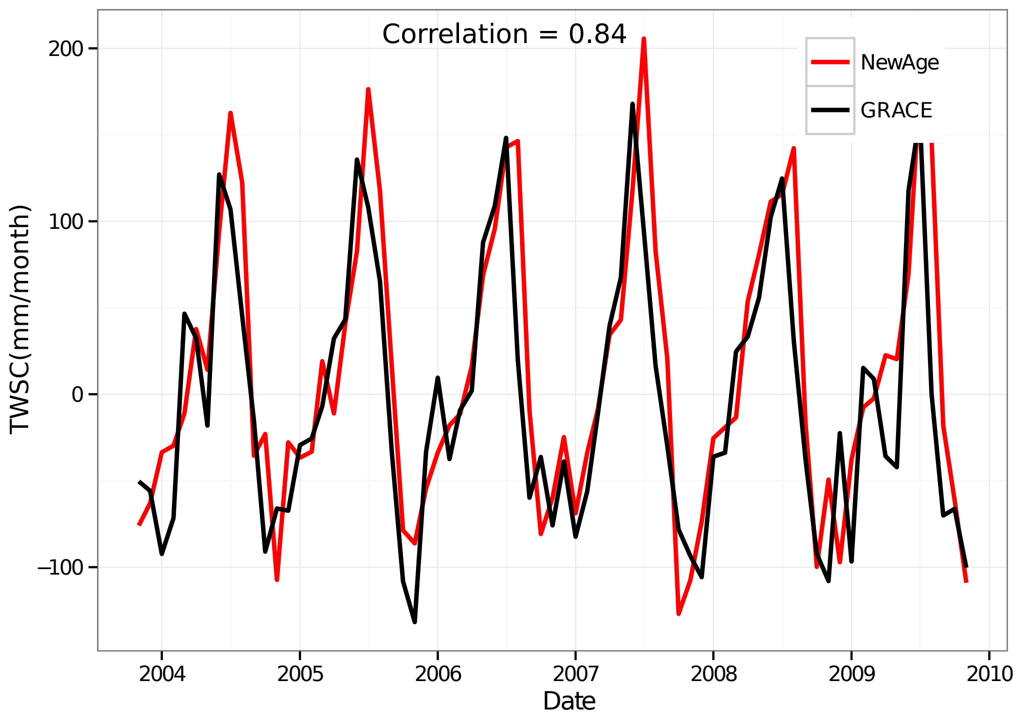

Figure 7. Comparison between basin-scale NewAge ds/dt and GRACE TWSC from 2004-2009 at monthly time steps.

5.2 Water budget closure

The water budget components (J, ET, Q, ds/dt) of 402 subbasin of the UBN are simulated for the period 1994-2009 at daily time steps. Figure 8 shows the long-term, monthly-mean, water budget closure derived from 1994-2009. The four months

Hydrol. Earth Syst. Sci. Discuss., doi:10.5194/hess-2016-290, 2016
Manuscript under review for journal Hydrol. Earth Syst. Sci.
Published: 20 June 2016

Hydrology and Earth System Sciences
Open Access
Discussions

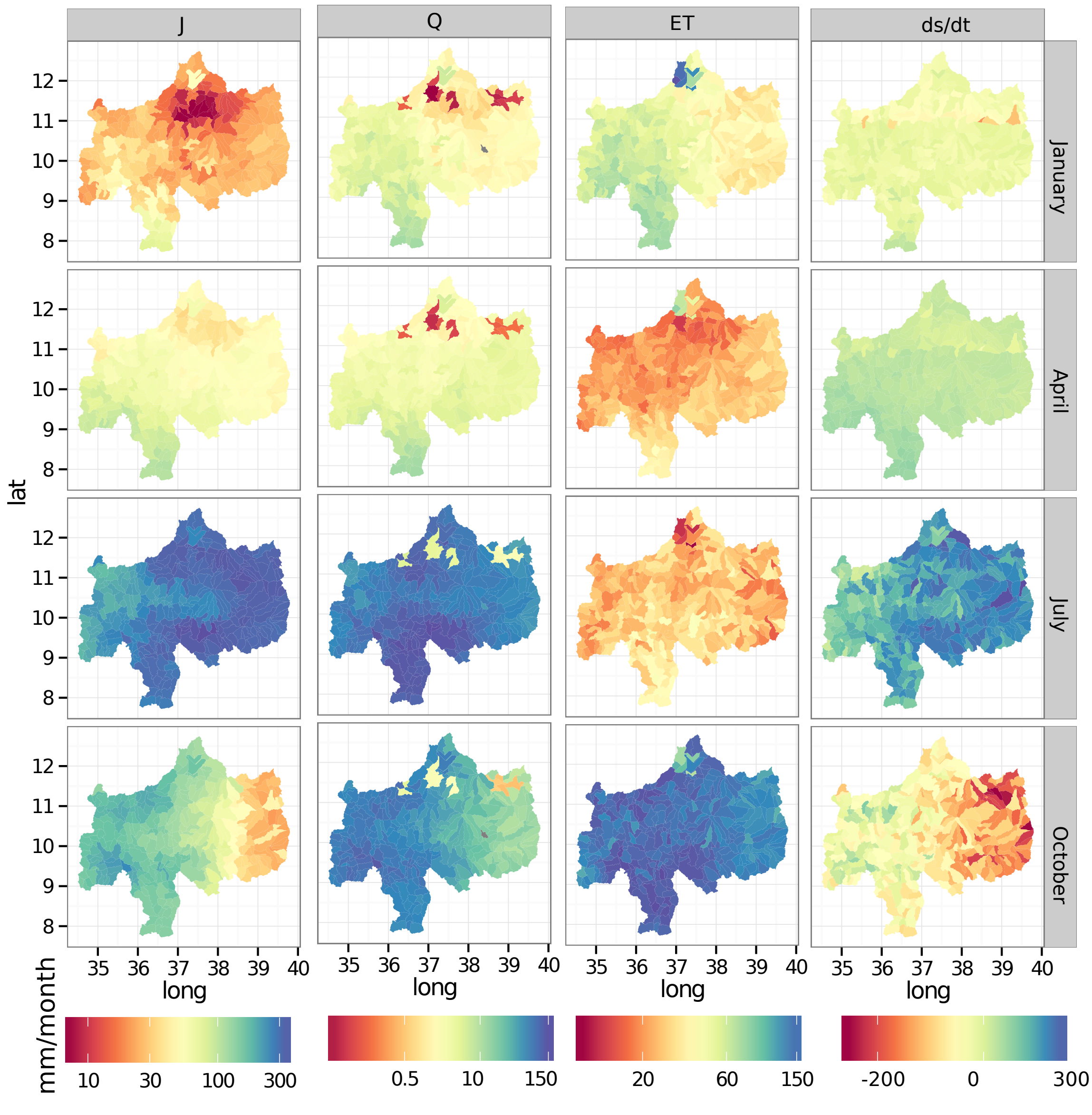

Figure 8. Spatial distribution of long term mean monthly water budget (January,April, July and October) in the UBN basin. For the sake of visibility, the legend is plotted separately and on logarithmic scale, except for the storage component.

Hydrology and Earth System Sciences
Open Access
Discussions

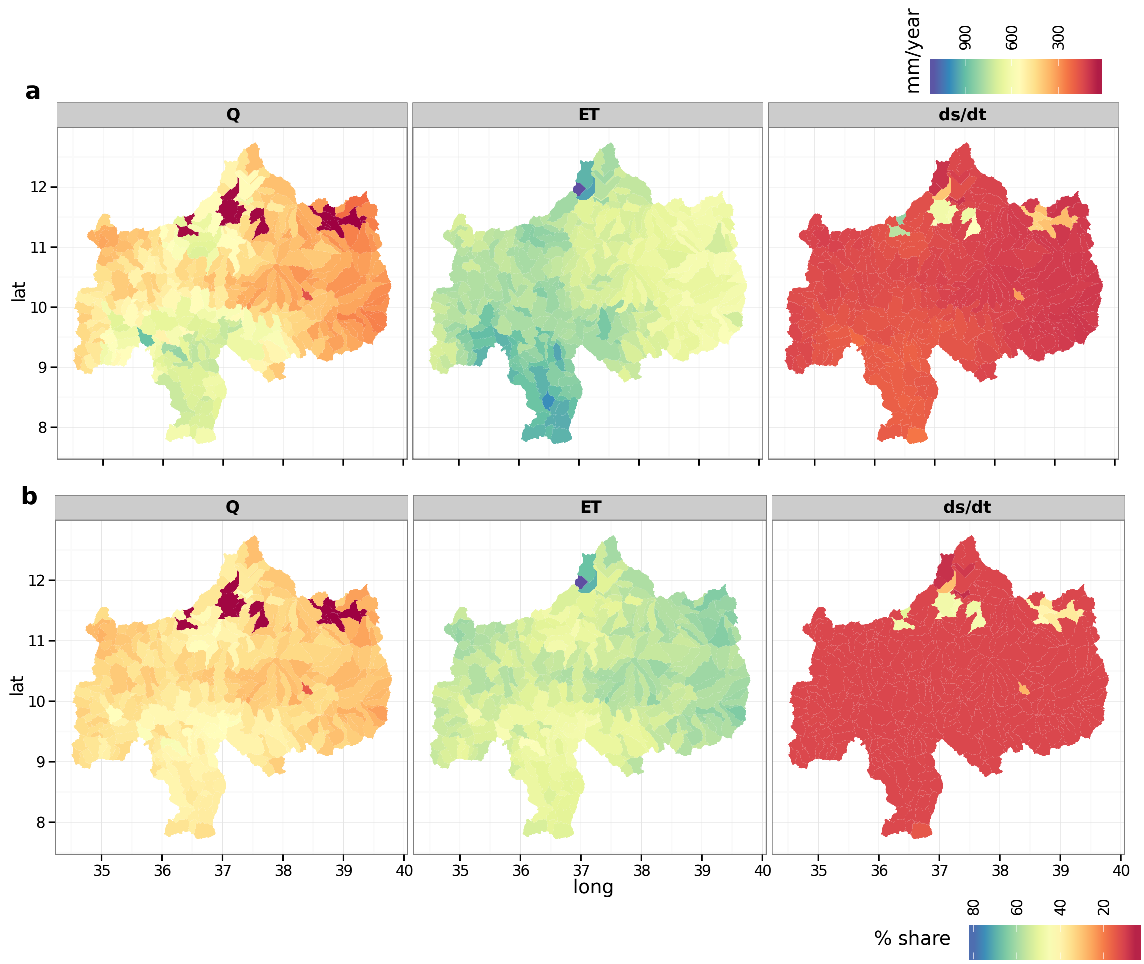

Figure 9. The spatial distributions of long term mean annual water budget closure: precipitation in mm (figure 3), the output terms (Q, ET, ds/dt) in mm (a), and the percentage share of the output term (Q, ET, ds/dt) of the total precipitation (b).

(January, April, July, and October) are selected to show the four seasons (Winter, Spring, Summer and Autumn). For all components, the mean seasonal variability is very high. Generally, the seasonal patterns of Q and ds/dt follow the J, showing the highest values in summer (i.e. July) and the lowest in winter (i.e. January). However, simulated ET shows distinct seasonal patterns with respect to the other components, the highest being during autumn (October), followed by winter (January). During the summer it is low, most likely due to high cloud cover.

The variability between the subbasins is also appreciable. Generally, all components tends to increase from the east to the southwest part of the basin, except for the summer season (July). During summer, on the other hand, the eastern part of the basin receives its highest rainfall, stores more water, and generates high runoff as well. In general the dominant budget component varies with months. For instance, in January ET is the dominant while in June and July ds/dt is more dominant. After the summer season, Q and ET are the dominant fluxes. A regression analysis based on the results for all subbasins and all years shows that, at short time scales such as at daily or monthly, the variability in ET is not due to variablity in J (R^2=0.01). Conversely, at the yearly time scale, 78% of ET variance is explained by variability in J.

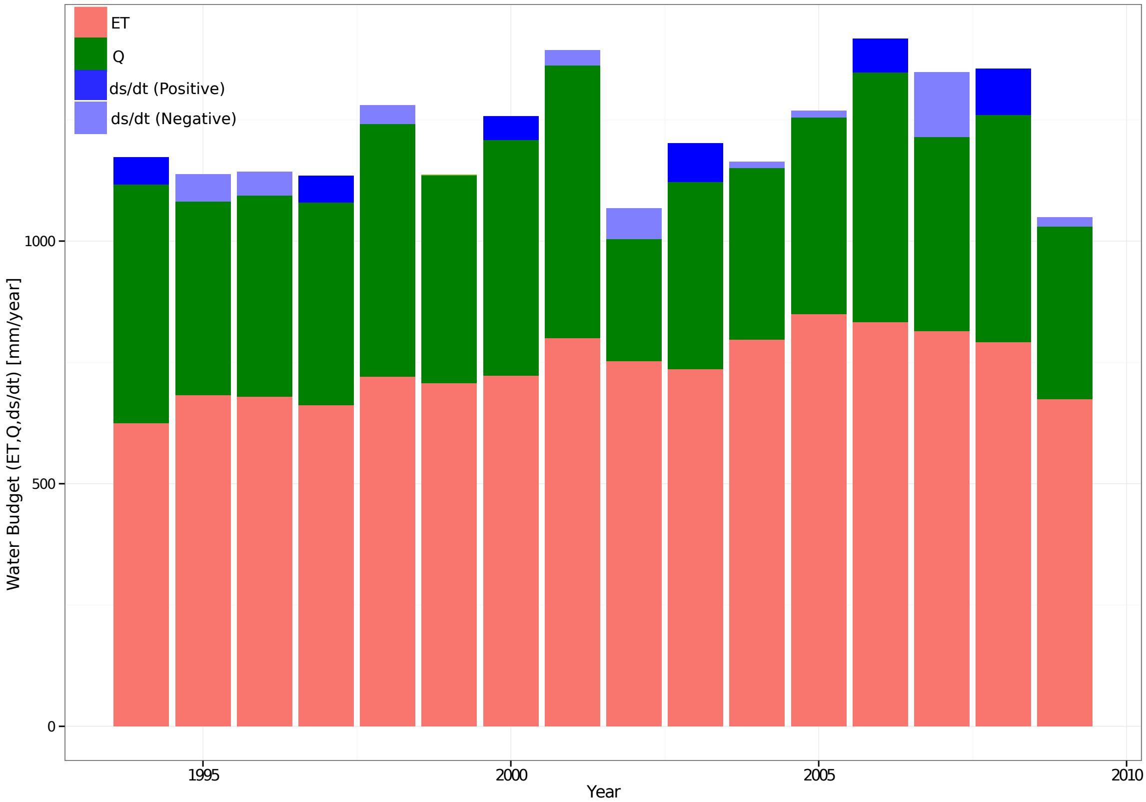

Figure 10. Water budget components of the basin and its annual variabilities from 1994 to 2009. The relative share of each of the three components (Q, ET and ds/dt) of the total available water J is represented by the length of the bars (N.B. the total length of the bar minus the negative storage is J). The positive and negative storage of the years are shown by dark blue and light blue respectively).

The spatial variability of the long term mean annual water budget closure is shown in figure 9. The spatial variability of J and Q is higher than ds/dt and ET. The higher Q and ET in the southern and southwestern part of the basin could be due to higher J. Similarly Q is lower in the eastern and northeastern part of the basin. Focusing on the percentage share of the output term (Q, ET, ds/dt) of total J (figure 9 c), ET dominates the water budget, followed by Q. It is noteworthy that the eastern subbasins with low ET still have percentage share of ET due to low amount of J received.

The long-term basin-average water budget components shows: 1360 $\pm$ 230 mm of J, followed by 740 $\pm$ 87 mm of ET, 454 $\pm$ 160 mm of Q and -4 $\pm$ 63 mm of S. While the spatial variability of the water budget is high, the annual variability is rather limited. Higher annual variability is observed for J, followed by Q. 2001 and 2006 are wet years, characterized by high J and Q. Conversely, 2002 and 2009 are dry years with 1167.480 mm and 1215.123 mm per year of precipitation. Details on the two dry years (2002, 2009) of the region can be consulted in Viste et al. (2013).

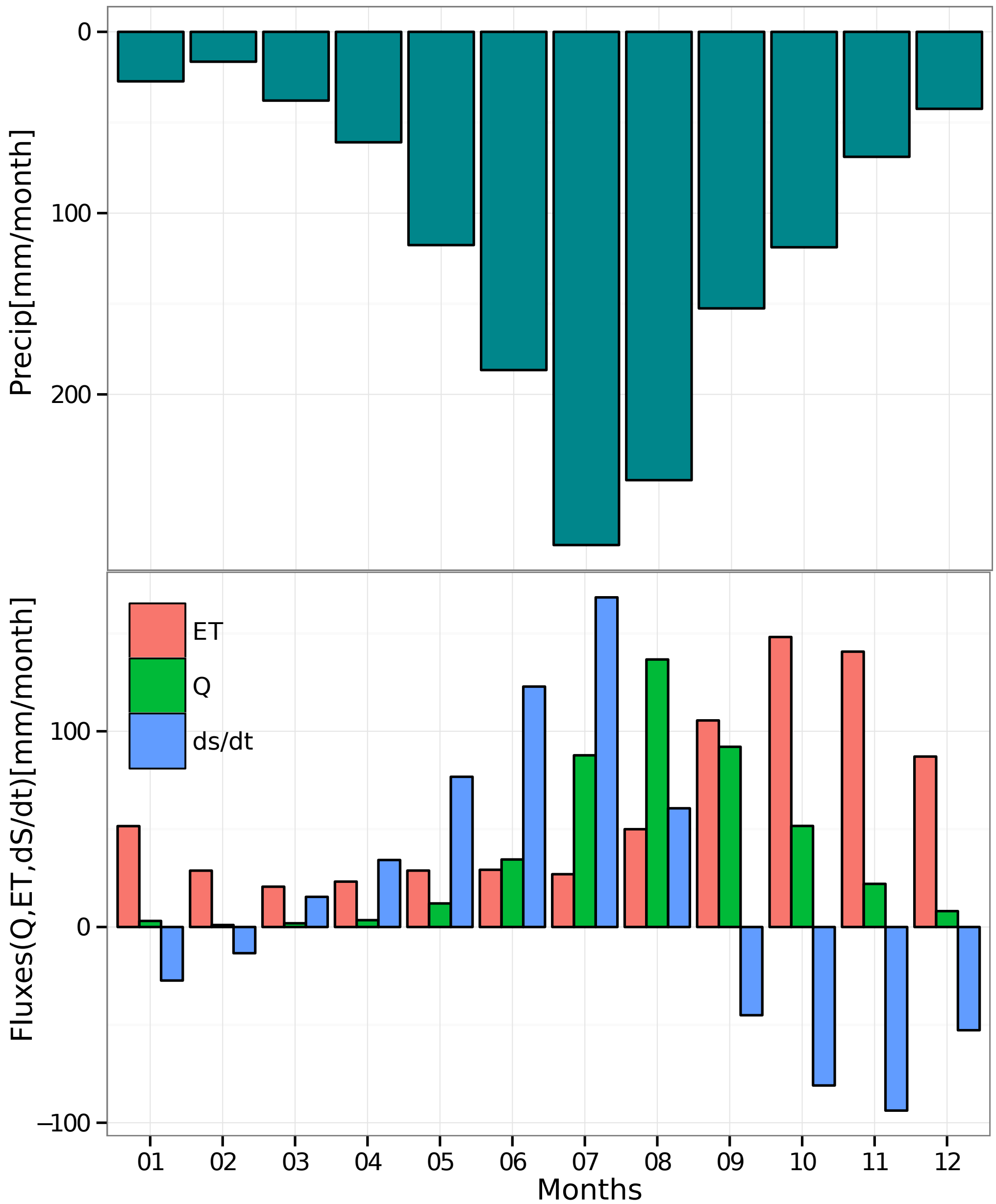

Figure 11. Monthly mean Water budget components at basin scale and long term, based on estimates from 1994 to 2009. The relative shares of the three components (Q, ET and dS/dt) of the total available water J are shown .

Figure 11 provides long term monthly mean estimates of water budget fluxes and storage. The basin scale mean budget is highly variable. The highest variability is mainly in J and S. During summer months, J, Q, and ds/dt shows high magnitude. ET is not highest in June, July and August, but, in October and December it is. The S accumulated in the summer season feeds the highest ET in autumn, and causes very high drops in S (figure 11).

6 Conclusions

The goal of this study is to estimate the whole water budget and its spatial and temporal variability using JGrass-NewAge hydrological model system and remote sensing data over the upper Blue Nile basin. The study covered 16 years from 1994-2009. Different remote sensing data are used to force and verify the modeling results. The results can be summarized as follows.

Different remote sensing data (SM2R-CCI, SAF EUMETSAT CFC, GLEAM, GRACE) are effectively employed either to force the water balance modelling or to verify model results. The performances of the modelling solution are promising (figure 5 and 7, and table 2) and often greatly improve previous results. The basin scale annual precipitation over the basin is 1360 $\pm$ 230 mm, and highly variable spatially. The southern and southwestern parts of the basin receive the highest precipitation, which tend to decrease towards the eastern parts of the basin (figure 3).

Generally, the interannual variability of ET is high, and tends to be higher in autumn and lower in summer). The average basin scale ET is about 740 $\pm$ 87 mm, and is the second most dominant component of water budget in the basin. The comparison of simulated ET with the satellite product GLEAM shows that GLEAM has low temporal variability. The correlation between GLEAM ET and NewAge ET increases from daily time steps to monthly time steps, and spatially it is higher in the east and central parts of the basin. Comparison with MODIS products was also performed (reported in complimentary material). MODIS actually shows even more large departure from JGrass-NewAGE results. Both satellite products, however, seem to introduce a systematic bias which would not allow to close the budget.

The NewAge ADIGE rainfall-runoff component is able to reproduce discharge very well at the outlet (KGE = 0.92). The long term annual runoff of the UBN basin is about 454 $\pm$ 160 mm. The verification results at the internal sites where measures are available reveal that the model can be used for forecasting at ungauged links with some success.

Generally, the long term water budget simulation shows that the basin is in equilibrium around zero storage (-4 $\pm$ 63 mm) with minor departures even after the 16 years at which the condition imposed by the Budiko hypothesis, i.e. $T_B = 6$ years could have been forgiven. The NewAge storage estimations and its space-time variability is effectively verified by the basin scale GRACE TWSC data and show high correlation and similar amplitude.

Reproducibility

The forcing data used for NewAge simulation: SM2R-CCI is obtained from http://hydrology.irpi.cnr.it/people/l.brocca; the rain gauge precipitation and hydrometer discharge data were obtained from the National meteorological Agency and Ministry of

Water and Energy of Ethiopia respectively, and it can be requested for research. The remote sensing data used for comparison: GLEAMS ET, MODIS ET and GRACE TWSC are freely available and can be downloaded at http://www.gleam.eu,http://www.ntsg.umt.edu/project/mod16, and ftp://podaac-ftp.jpl.nasa.gov/allData/tellus/L3/landmass/RL05 respectively. Modelling components used for the simulations are available and documented through the Geoframe blog http:geoframe.blogspot.com.

Acknowledgements. This research has been partially financed by the CLIMAWARE projects of University of Trento (/http://abouthydrology.blogspot.it/search/label/CLIMAWARE) and by European Union FP7 Collaborative Project GLOBAQUA (Managing the effects of multiple stressors on aquatic ecosystems under water scarcity, grant no. 603629-ENV-2013.6.2.1). We would like to acknowledge the National meteorological Agency and Ministry of Water and Energy of Ethiopia for providing us the gauge rainfall and discharge data.

Appendix A: Model performance criteria

The model evaluation statistics used in the paper are the goodness-of-fit (GOF) indices. The following indexes are used as objective function and comparison of estimations.

1. PBIAS: is the measure of average tendency of estimated values to be large or smaller that their measured values. The value near to zero indicates high estimation, whereas the positive value indicates the overestimation and negative values indicate model underestimation (Moriasi et al., 2007; Gupta et al., 1999).

$$PBIAS = \frac{\sum_{i=1}^{n}(P_i - O_i)}{\sum_{i=1}^{n} O_i} 100 \tag{A1}$$

The PBIAS value ranges from -20 to 20% is considered good, and values between ±20% and ±40% and those greater than ±40% are considered satisfactory and unsatisfactory respectively (Stehr et al., 2008).

2. Kling-Gupta efficiency (KGE) is developed by Gupta et al. (2009) to provide a diagnostically interesting decomposition of the Nash-Sutcliffe efficiency (and hence MSE), which facilitates the analysis of the relative importance of its different components (correlation, bias and variability) in the context of hydrological modelling. Kling et al. (2012) proposed a revised version of this index. It is given by

$$KGE = 1 - ED \tag{A2}$$

$$ED = \sqrt{(r-1)^2 + (vr-1)^2 + (\beta-1)^2} \tag{A3}$$

where ED is the Euclidian distance from the ideal point, β is the ratio between the mean simulated and mean observed flows, r is Pearson product-moment correlation coefficient, and v is the ratio between the observed (σ_o) and modelled

Hydrol. Earth Syst. Sci. Discuss., doi:10.5194/hess-2016-290, 2016
Manuscript under review for journal Hydrol. Earth Syst. Sci.
Published: 20 June 2016

(σ_s) standard deviations of the time series and takes account of the relative variability (Zambrano-Bigiarini, 2013). The KGE ranges from infinity to a perfect estimation of 1, but a performance above 0.75 and 0.5 is considered as good and intermediate respectively (Thiemig et al., 2013).

3. Pearson correlation coefficient (r): please refer Moriasi et al. (2007). The correlation coefficient is best as much as it is close to 1.

References

Abera, W., Antonello, A., Franceschi, S., Formetta, G., and Rigon, R.: The uDig Spatial Toolbox for hydro-geomorphic analysis, British Society for Geomorphology, London, UK, in: clarke & nield (eds.) geomorphological techniques (online edition) edn., 2014.

Abera, W., Brocca, L., and Rigon, R.: Comparative evaluation of different satellite rainfall estimation products and bias correction in the Upper Blue Nile (UBN) basin, Atmospheric Research, 2016.

Abera, W., Formetta, G., Brocca, L., and Rigon, R.: Estimating water budgets and their variability of snow-dominated, Pri-Alpine small basin with NewAge-JGrass, HESSD, submitted.

Abtew, W., Melesse, A. M., and Dessalegne, T.: Spatial, inter and intra-annual variability of the Upper Blue Nile Basin rainfall, Hydrological processes, 23, 3075–3082, 2009.

Abu-Zeid, M. A. and Biswas, A. K.: River basin planning and management, Oxford University Press, 1996.

Andrew, M. E., Wulder, M. A., and Nelson, T. A.: Potential contributions of remote sensing to ecosystem service assessments, Progress in Physical Geography, 38, 328–353, 2014.

Arking, A.: The radiative effects of clouds and their impact on climate, Bulletin of the American Meteorological Society, 72, 795–813, 1991.

Assouline, S., Li, D., Tyler, S., Tanny, J., Cohen, S., Bou-Zeid, E., Parlange, M., and Katul, G. G.: On the variability of the Priestley-Taylor coefficient over water bodies, Water Resources Research, 2016.

Bellerby, T.: Satellite rainfall uncertainty estimation using an artificial neural network, Journal of Hydrometeorology, 8, 1397–1412, 2007.

Bewket, W. and Sterk, G.: Dynamics in land cover and its effect on stream flow in the Chemoga watershed, Blue Nile basin, Ethiopia, Hydrological Processes, 19, 445–458, 2005.

Billah, M. M., Goodall, J. L., Narayan, U., Reager, J., Lakshmi, V., and Famiglietti, J. S.: A methodology for evaluating evapotranspiration estimates at the watershed-scale using GRACE, Journal of Hydrology, 523, 574–586, 2015.

Block, P. and Rajagopalan, B.: Interannual variability and ensemble forecast of Upper Blue Nile Basin Kiremt season precipitation, Journal of Hydrometeorology, 8, 327–343, 2007.

Brocca, L., Moramarco, T., Melone, F., and Wagner, W.: A new method for rainfall estimation through soil moisture observations, Geophysical Research Letters, 40, 853–858, 2013.

Brocca, L., Ciabatta, L., Massari, C., Moramarco, T., Hahn, S., Hasenauer, S., Kidd, R., Dorigo, W., Wagner, W., and Levizzani, V.: Soil as a natural rain gauge: estimating global rainfall from satellite soil moisture data, Journal of Geophysical Research: Atmospheres, 119, 5128–5141, 2014.

Budyko, M.: 1., 1974: Climate and Life, International Geophysics Series, 18, 1978.

Camberlin, P.: Rainfall anomalies in the source region of the Nile and their connection with the Indian summer monsoon, Journal of Climate, 10, 1380–1392, 1997.

Conway, D.: A water balance model of the Upper Blue Nile in Ethiopia, Hydrological sciences journal, 42, 265–286, 1997.

Conway, D.: The climate and hydrology of the Upper Blue Nile River, Geographical Journal, pp. 49–62, 2000.

Conway, D.: From headwater tributaries to international river: observing and adapting to climate variability and change in the Nile basin, Global Environmental Change, 15, 99–114, 2005.

Conway, D. and Hulme, M.: Recent fluctuations in precipitation and runoff over the Nile sub-basins and their impact on main Nile discharge, Climatic change, 25, 127–151, 1993.

Hydrology and Earth System Sciences
Discussions

Döll, P., Fritsche, M., Eicker, A., and Schmied, H. M.: Seasonal water storage variations as impacted by water abstractions: comparing the output of a global hydrological model with GRACE and GPS observations, Surveys in Geophysics, 35, 1311–1331, 2014.

Easton, Z., Fuka, D., White, E., Collick, A., Biruk Ashagre, B., McCartney, M., Awulachew, S., Ahmed, A., and Steenhuis, T.: A multi basin SWAT model analysis of runoff and sedimentation in the Blue Nile, Ethiopia, Hydrology and earth system sciences, 14, 1827–1841, 2010.

Fisher, J. B., Tu, K. P., and Baldocchi, D. D.: Global estimates of the land–atmosphere water flux based on monthly AVHRR and ISLSCP-II data, validated at 16 FLUXNET sites, Remote Sensing of Environment, 112, 901–919, 2008.

Formetta, G.: Hydrological modelling with components: the OMS3 NewAge-JGrass system, Ph.D. thesis, University of Trento, 2013.

Formetta, G., Mantilla, R., Franceschi, S., Antonello, A., and Rigon, R.: The JGrass-NewAge system for forecasting and managing the hydrological budgets at the basin scale: models of flow generation and propagation/routing, Geoscientific Model Development, 4, 943–955, 2011.

Formetta, G., Rigon, R., Chávez, J., and David, O.: Modeling shortwave solar radiation using the JGrass-NewAge system, Geoscientific Model Development, 6, 915–928, 2013.

Formetta, G., Antonello, A., Franceschi, S., David, O., and R., R.: The basin delineation and the built of a digital watershed model within the JGrass-NewAGE system, Bolet?n Geol?gico y Minero: Special Issue "Advanced GIS terrain analysis for geophysical applications, 2014a.

Formetta, G., Antonello, A., Franceschi, S., David, O., and Rigon, R.: Hydrological modelling with components: A GIS-based open-source framework, Environmental Modelling & Software, 55, 190–200, 2014b.

Formetta, G., Kampf, S. K., David, O., and Rigon, R.: Snow water equivalent modeling components in NewAge-JGrass, Geoscientific Model Development, 7, 725–736, 2014c.

Gao, H., Tang, Q., Ferguson, C. R., Wood, E. F., and Lettenmaier, D. P.: Estimating the water budget of major US river basins via remote sensing, International Journal of Remote Sensing, 31, 3955–3978, 2010.

Gebremicael, T., Mohamed, Y., Betrie, G., van der Zaag, P., and Teferi, E.: Trend analysis of runoff and sediment fluxes in the Upper Blue Nile basin: A combined analysis of statistical tests, physically-based models and landuse maps, Journal of Hydrology, 482, 57–68, 2013.

Gupta, H. V., Sorooshian, S., and Yapo, P. O.: Status of automatic calibration for hydrologic models: Comparison with multilevel expert calibration, Journal of Hydrologic Engineering, 4, 135–143, 1999.

Gupta, H. V., Kling, H., Yilmaz, K. K., and Martinez, G. F.: Decomposition of the mean squared error and NSE performance criteria: Implications for improving hydrological modelling, Journal of Hydrology, 377, 80–91, 2009.

Hall, J., Grey, D., Garrick, D., Fung, F., Brown, C., Dadson, S., Sadoff, C., et al.: Coping with the curse of freshwater variability, Science, 346, 429–430, 2014.

Hong, Y., Hsu, K.-l., Moradkhani, H., and Sorooshian, S.: Uncertainty quantification of satellite precipitation estimation and Monte Carlo assessment of the error propagation into hydrologic response, Water resources research, 42, 2006.

Huffman, G. J., Bolvin, D. T., Nelkin, E. J., Wolff, D. B., Adler, R. F., Gu, G., Hong, Y., Bowman, K. P., and Stocker, E. F.: The TRMM multisatellite precipitation analysis (TMPA): Quasi-global, multiyear, combined-sensor precipitation estimates at fine scales, Journal of Hydrometeorology, 8, 38–55, 2007.

Jarmain, C.: A Methodology for Near-real Time Spatial Estimation of Evaporation: Report to the Water Research Commission, Water Research Commission, 2009.

Johnston, R. M. and McCartney, M.: Inventory of water storage types in the Blue Nile and Volta river basins, vol. 140, IWMI, 2010.

Joyce, R. J., Janowiak, J. E., Arkin, P. A., and Xie, P.: CMORPH: A method that produces global precipitation estimates from passive microwave and infrared data at high spatial and temporal resolution, Journal of Hydrometeorology, 5, 487–503, 2004.

Karlsson, K.-G., Riihelä, A., Müller, R., Meirink, J., Sedlar, J., Stengel, M., Lockhoff, M., Trentmann, J., Kaspar, F., Hollmann, R., et al.: CLARA-A1: a cloud, albedo, and radiation dataset from 28 yr of global AVHRR data, Atmospheric Chemistry and Physics, 13, 5351–5367, 2013.

Kebede, S., Travi, Y., Alemayehu, T., and Marc, V.: Water balance of Lake Tana and its sensitivity to fluctuations in rainfall, Blue Nile basin, Ethiopia, Journal of hydrology, 316, 233–247, 2006.

Kennedy, J., Eberhart, R., et al.: Particle swarm optimization, in: Proceedings of IEEE international conference on neural networks, vol. 4, pp. 1942–1948, Perth, Australia, 1995.

Kim, J. and Hogue, T. S.: Evaluation of a MODIS-based potential evapotranspiration product at the point scale, Journal of Hydrometeorology, 9, 444–460, 2008.

Kim, U. and Kaluarachchi, J. J.: Application of parameter estimation and regionalization methodologies to ungauged basins of the Upper Blue Nile River Basin, Ethiopia, Journal of Hydrology, 362, 39–56, 2008.

Kim, U. and Kaluarachchi, J. J.: Climate change impacts on water resources in the Upper Blue Nile River Basin, Ethiopia1, 2009.

Kim, U., Kaluarachchi, J. J., and Smakhtin, V. U.: Generation of monthly precipitation under climate change for the upper blue Nile river basin, Ethiopia1, 2008.

Kjaersgaard, J., Allen, R., Garcia, M., Kramber, W., and Trezza, R.: Automated selection of anchor pixels for landsat based evapotranspiration estimation, American Society of Civil Engineers, Kansas City, Missouri, 2009.

Kjærsgaard, J. H., Cuenca, R. H., Martínez-Cob, A., Gavilán, P., Plauborg, F., Mollerup, M., and Hansen, S.: Comparison of the performance of net radiation calculation models, Theoretical and applied climatology, 98, 57–66, 2009.

Kling, H., Fuchs, M., and Paulin, M.: Runoff conditions in the upper Danube basin under an ensemble of climate change scenarios, Journal of Hydrology, 424, 264–277, 2012.

Kummerow, C., Barnes, W., Kozu, T., Shiue, J., and Simpson, J.: The tropical rainfall measuring mission (TRMM) sensor package, Journal of atmospheric and oceanic technology, 15, 809–817, 1998.

Landerer, F. and Swenson, S.: Accuracy of scaled GRACE terrestrial water storage estimates, Water Resources Research, 48, 2012.

McCabe, M. F., Ershadi, A., Jimenez, C., Miralles, D., Michel, D., and Wood, E. F.: The GEWEX LandFlux project: evaluation of model evaporation using tower-based and globally gridded forcing data, Geoscientific Model Development, 9, 283–305, 2016.

Mellander, P.-E., Gebrehiwot, S. G., Gardenas, A. I., Bewket, W., and Bishop, K.: Summer rains and dry seasons in the Upper Blue Nile Basin: the predictability of half a century of past and future spatiotemporal patterns, PloS one, 8, 1932–6203, 2013.

Mengistu, D. and Sorteberg, A.: Sensitivity of SWAT simulated streamflow to climatic changes within the Eastern Nile River basin, Hydrology and Earth System Sciences, 16, 391–407, 2012.

Michelangeli, P.-A., Vrac, M., and Loukos, H.: Probabilistic downscaling approaches: Application to wind cumulative distribution functions, Geophysical Research Letters, 36, 2009.

Miralles, D., Holmes, T., De Jeu, R., Gash, J., Meesters, A., and Dolman, A.: Global land-surface evaporation estimated from satellite-based observations, Hydrology and Earth System Sciences, 15, 453–469, 2011a.

Miralles, D. G., De Jeu, R. A. M., Gash, J. H., Holmes, T. R. H., and Dolman, A. J.: Magnitude and variability of land evaporation and its components at the global scale, Hydrology and Earth System Sciences, 15, 967–981, doi:10.5194/hess-15-967-2011, http://www.hydrol-earth-syst-sci.net/15/967/2011/, 2011b.

Mishra, A. and Hata, T.: A grid-based runoff generation and flow routing model for the upper Blue Nile basin, Hydrological sciences journal, 51, 191–206, 2006.

Mishra, A., Hata, T., and Abdelhadi, A.: Models for recession flows in the upper Blue Nile River, Hydrological processes, 18, 2773–2786, 2004.

Moore, R.: The probability-distributed principle and runoff production at point and basin scales, Hydrological Sciences Journal, 30, 273–297, 1985.

Moriasi, D., Arnold, J., Van Liew, M., Bingner, R., Harmel, R., and Veith, T.: Model evaluation guidelines for systematic quantification of accuracy in watershed simulations, Trans. ASABE, 50, 885–900, 2007.

Mu, Q., Heinsch, F. A., Zhao, M., and Running, S. W.: Development of a global evapotranspiration algorithm based on MODIS and global meteorology data, Remote Sensing of Environment, 111, 519–536, 2007.

Nash, J. E. and Sutcliffe, J. V.: River flow forecasting through conceptual models part I—A discussion of principles, Journal of hydrology, 10, 282–290, 1970.

Norman, J. M., Kustas, W. P., and Humes, K. S.: Source approach for estimating soil and vegetation energy fluxes in observations of directional radiometric surface temperature, Agricultural and Forest Meteorology, 77, 263–293, 1995.

Pejam, M., Arain, M., and McCaughey, J.: Energy and water vapour exchanges over a mixedwood boreal forest in Ontario, Canada, Hydrological Processes, 20, 3709–3724, 2006.

Pimentel, D., Berger, B., Filiberto, D., Newton, M., Wolfe, B., Karabinakis, E., Clark, S., Poon, E., Abbett, E., and Nandagopal, S.: Water resources: agricultural and environmental issues, BioScience, 54, 909–918, 2004.

Priestley, C. and Taylor, R.: On the assessment of surface heat flux and evaporation using large-scale parameters, Monthly weather review, 100, 81–92, 1972.

Rientjes, T., Haile, A., Kebede, E., Mannaerts, C., Habib, E., and Steenhuis, T.: Changes in land cover, rainfall and stream flow in Upper Gilgel Abbay catchment, Blue Nile basin–Ethiopia, Hydrology and Earth System Sciences, 15, 1979–1989, 2011.

Sahoo, A. K., Pan, M., Troy, T. J., Vinukollu, R. K., Sheffield, J., and Wood, E. F.: Reconciling the global terrestrial water budget using satellite remote sensing, Remote Sensing of Environment, 115, 1850–1865, 2011.

Schaefli, B. and Gupta, H. V.: Do Nash values have value?, Hydrological Processes, 21, 2075–2080, 2007.

Scheerlinck, K., Pauwels, V., Vernieuwe, H., and De Baets, B.: Calibration of a water and energy balance model: Recursive parameter estimation versus particle swarm optimization, Water resources research, 45, 2009.

Schulz, J., Albert, P., Behr, H.-D., Caprion, D., Deneke, H., Dewitte, S., Dürr, B., Fuchs, P., Gratzki, A., Hechler, P., et al.: Operational climate monitoring from space: the EUMETSAT Satellite Application Facility on Climate Monitoring (CM-SAF)., Atmospheric Chemistry & Physics, 9, 2009.

Seleshi, Y. and Zanke, U.: Recent changes in rainfall and rainy days in Ethiopia, International journal of climatology, 24, 973–983, 2004.

Setegn, S. G., Srinivasan, R., and Dargahi, B.: Hydrological modelling in the Lake Tana Basin, Ethiopia using SWAT model, The Open Hydrology Journal, 2, 2008.

Sheffield, J., Ferguson, C. R., Troy, T. J., Wood, E. F., and McCabe, M. F.: Closing the terrestrial water budget from satellite remote sensing, Geophysical Research Letters, 36, 2009.

Sheffield, J., Wood, E. F., and Roderick, M. L.: Little change in global drought over the past 60 years, Nature, 491, 435–438, 2012.

Sorooshian, S., Hsu, K.-L., Gao, X., Gupta, H. V., Imam, B., and Braithwaite, D.: Evaluation of PERSIANN system satellite-based estimates of tropical rainfall, Bulletin of the American Meteorological Society, 81, 2035–2046, 2000.

Steenhuis, T. S., Collick, A. S., Easton, Z. M., Leggesse, E. S., Bayabil, H. K., White, E. D., Awulachew, S. B., Adgo, E., and Ahmed, A. A.: Predicting discharge and sediment for the Abay (Blue Nile) with a simple model, Hydrological processes, 23, 3728–3737, 2009.

Stehr, A., Debels, P., Romero, F., and Alcayaga, H.: Hydrological modelling with SWAT under conditions of limited data availability: evaluation of results from a Chilean case study, Hydrological sciences journal, 53, 588–601, 2008.

Swenson, S. and Wahr, J.: Post-processing removal of correlated errors in GRACE data, Geophysical Research Letters, 33, 2006.

Taye, M. T. and Willems, P.: Influence of climate variability on representative QDF predictions of the upper Blue Nile basin, Journal of hydrology, 411, 355–365, 2011.

Teferi, E., Uhlenbrook, S., Bewket, W., Wenninger, J., and Simane, B.: The use of remote sensing to quantify wetland loss in the Choke Mountain range, Upper Blue Nile basin, Ethiopia, Hydrology and Earth System Sciences, 14,(12), 2010.

Tekleab, S., Uhlenbrook, S., Mohamed, Y., Savenije, H., Temesgen, M., and Wenninger, J.: Water balance modeling of Upper Blue Nile catchments using a top-down approach, Hydrology and Earth System Sciences, 15,(7), 2011.

Thiemig, V., Rojas, R., Zambrano-Bigiarini, M., and De Roo, A.: Hydrological evaluation of satellite-based rainfall estimates over the Volta and Baro-Akobo Basin, Journal of Hydrology, 499, 324–338, 2013.

Uhlenbrook, S., Mohamed, Y., and Gragne, A.: Analyzing catchment behavior through catchment modeling in the Gilgel Abay, upper Blue Nile River basin, Ethiopia, Hydrology and Earth System Sciences, 14, 2153–2165, 2010.

Viste, E., Korecha, D., and Sorteberg, A.: Recent drought and precipitation tendencies in Ethiopia, Theoretical and Applied Climatology, 112, 535–551, 2013.

Wale, A., Rientjes, T., Gieske, A., and Getachew, H.: Ungauged catchment contributions to Lake Tana's water balance, Hydrological processes, 23, 3682–3693, 2009.

Wang, H., Guan, H., Gutiérrez-Jurado, H. A., and Simmons, C. T.: Examination of water budget using satellite products over Australia, Journal of Hydrology, 511, 546–554, 2014.

Wosenie, M. D., Verhoest, N., Pauwels, V., Negatu, T. A., Poesen, J., Adgo, E., Deckers, J., and Nyssen, J.: Analyzing runoff processes through conceptual hydrological modeling in the Upper Blue Nile Basin, Ethiopia, Hydrology and Earth System Sciences, 18, 5149–5167, 2014.

Zambrano-Bigiarini, M.: hydroGOF: Goodness-of-fit functions for comparison of simulated and observed hydrological time series, R package version 0.3-7, 2013.